Passive, Adaptive, Active Vibration Control, and Integrated Approaches

Dirk Mayer and Sven Herold

Additional information is available at the end of the chapter

Abstract

Passive vibration control solutions like tuned vibration absorbers are often limited to tackle a single structural resonance or a specific disturbance frequency. Active vibration control systems can overcome these limitations, yet requiring continuously electrical energy for a sufficient performance. Thus, in some cases, a passive vibration control system is still preferable. Yet, the integration of active elements enables adaptation of the system parameters, for instance, the resonance of a tuned vibration absorber. These adaptive or semi-active systems only require external energy for the adaptation, while the compensating forces are generated by the inertia of the absorber's mass. In this contribution, the fundamentals of active, passive, and adaptive vibration control are briefly summarized and compared regarding their main advantages and design challenges. In the second part, a design of an inertial mass device with integrated piezoelectric actuators is presented. By applying a lever mechanism, the stiffness of the inertial mass device can be tuned even to very low frequencies. The device can be used to implement both adaptive tuned vibration absorbers and active control systems. In the last section of the chapter, the device is used in an experiment for vibration control of a large elastic structure. The setup is used to demonstrate different strategies for the realization of a vibration control system and the integration of different vibration control strategies.

Keywords: vibration control, active vibration control, passive vibration control, piezoelectric actuators, adaptive vibration absorbers

1. Introduction

Tuned vibration absorbers (TVA) and tuned mass dampers (TMD) are used since the beginning of the twentieth century to reduce disturbing vibrations [1]. Basically, this method uses an inertial mass that is elastically coupled to the vibrating host structure [2]. This resonant spring-mass

system can be tuned to certain resonance frequencies of the host structure (**Figure 1**). Then, the device is usually referred to as tuned mass damper (TMD), which is frequently applied to elastic infrastructure objects like towers or bridges. For large objects, several TMDs are distributed among the structure [3].

When the oscillator is tuned to a harmonic disturbance frequency, it is called tuned vibration absorber or vibration neutralizer [4]. Potential applications range from Optical Disc Drives, using an absorber mass of about 40 g [5] to vibrations of ship engines, requiring over 10 tons of oscillating mass [6]. The performance of these devices is mainly limited by the precise tuning to the target frequency. If a certain bandwidth is to be tackled, a high inertial mass has to be used, which usually prevents the application of TVAs in such cases.

In this chapter, several improvements to the traditional passive vibration absorber are introduced that have been made over the last decades, ranging from semi-active or adaptive to active dynamic systems (**Figure 2**).

In the next section, the basics of the different vibration control systems are summarized and examples for realized systems are given. In the last two sections, a system that can be used for
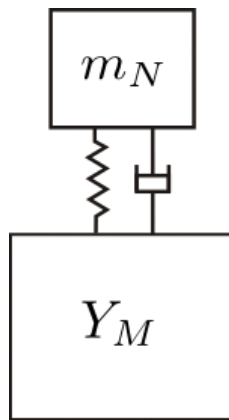
Figure 1. Generic vibration control set up with a passive TVA.
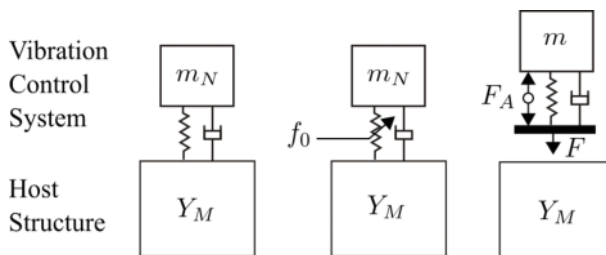
Figure 2. Vibration control systems—passive, adaptive, and active.

adaptive and active vibration control methods is presented and the application to an elastic vibrating structure is investigated.

2. Passive, adaptive, and active vibration control systems

2.1. Passive vibration control with tuned vibration absorbers

To illustrate the working principle of a passive TVA, the generic example from **Figure 1** is studied. The vibrating host structure is represented by a mechanical mobility Y_M. If the structure can be treated as a vibrating mass element of mass M, i.e., away from its resonance frequencies, the mobility reads [7]:

$$Y_m(s) = \frac{1}{sM} \tag{1}$$

The neutralizer is described by its mass m_N, resonance frequency ω_0, and damping coefficient θ. Then, its input mobility at the base can be derived to:

$$Y_N(s) = \frac{1}{m_N} \frac{s^2 + s\,2\,\theta\omega_0 + \omega_0^2}{s^2 2\,\theta\omega_0 + s\,\omega_0^2} \tag{2}$$

The connection of both systems is represented by:

$$Y(s) = \frac{Y_m(s)Y_N(s)}{Y_m(s) + Y_N(s)} = \frac{s^2 + s\,2\,\theta\omega_0 + \omega_0^2}{sM\left(s^2 + s2\theta\omega_0 + \omega_0^2\right) + m_N\left(s\omega_0^2 + s^2 2\theta\omega_0^2\right)} \tag{3}$$

Obviously, the mobility transfer function has a pair of conjugated complex zeros that match the resonance of the TVA. If the TVA is fully undamped, the mobility of the system at the resonance of the TVA turns to zero, i.e., complete cancellation of vibrations. It can be shown that the performance of the passive TVA is directly proportional to the mass ratio m_N/M, while increased damping has the contrary effect [8]. This issue is illustrated in **Figure 3** (left). Also the bandwidth of the absorption effect increases with a larger absorber mass. However, in most practical applications, a mass ratio of ½ will not be acceptable, so the passive TVA is restricted to situations where the disturbance frequency is known to be constant over time or where the added mass of a heavy TVA does not matter.

When the relevant frequency range of the host structure contains a resonance, the mobility formulation for Y_m becomes:

$$Y_m = \frac{s}{s^2 M + 2\theta_H\,\omega_{0,H}\,s + \omega_{0,H}^2}, \tag{4}$$

where $\omega_{0,H}$ is the resonance and θ_H is the damping coefficient of the host structure. The TVA is then used as a Tuned Mass Damper (TMD). The main difference is that a significant damping is needed to reach optimal vibration control performance [2]. This effect is demonstrated in
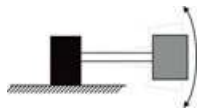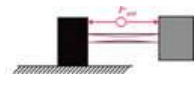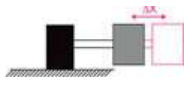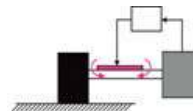
Figure 3 (right). Also, the TMD is usually designed with a lower mass ratio. In the given example, a ratio of $\frac{m_N}{M} = 0.1$ already provides a sufficient vibration reduction performance. It should be noted that the formulae for optimal tuning of a TMD are restricted for the application example of a single-degree-of-freedom oscillator excited by a harmonic force. In case of other excitation mechanisms like base acceleration, which is relevant for seismic vibration reduction, other TMD parameter values might provide the optimal vibration reduction performance [9]. For structures with several resonances or larger objects which cannot be treated as simple point mass oscillators any more, the design of distributed TMD systems requires some advanced methods like numerical optimization [3].

2.2. Adaptive tuned vibration absorbers

Adaptive tuned vibration absorbers have been proposed to overcome this weakness of passive TVAs. By using actuating elements, the resonance frequency of the absorber can be adjusted. In turn, an adaptive TVA can be designed with a smaller inertial mass [10]. In the last decades, numerous concepts have been investigated [11–14], but the designs can be traced back to some basic principles of adaptation [15] (**Table 1**).
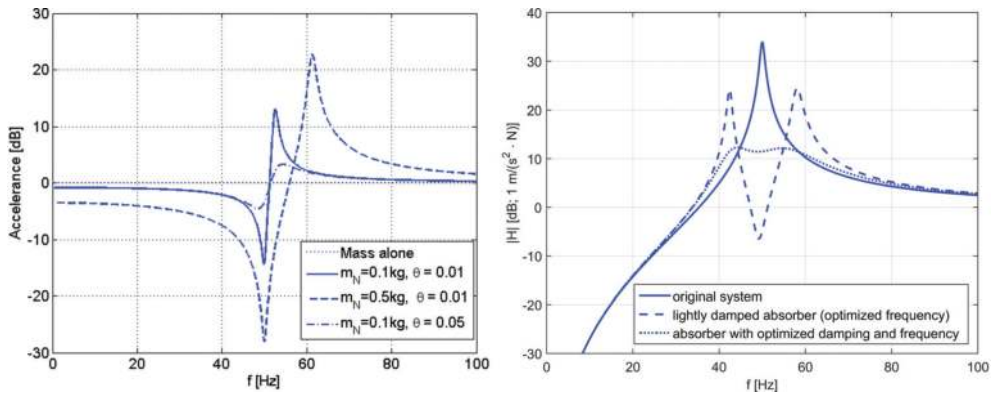
Figure 3. Accelerance of a 1 kg mass with a TVA tuned to 50 Hz (left); and a 50 Hz mass-spring-system with a TMD (right).

Concept	Static prestress	Variable geometry	Dynamic forces
Actuator principle	Static – high force	Static – high stroke	Dynamic force actuator
Actuator types	Motor, piezoelectric,…	Motor, shape memory alloy wires,…	Piezoelectric, electrodynamic

Table 1. Basic concepts for the realization of adaptive tuned vibration absorbers [15].

A common approach to alter the resonance frequency of a mechanical oscillator is the adjustment of the mechanical stiffness via the geometry of the spring element; for instance, by moving the inertial mass on a bending beam, which adjusts the effective beam length, as demonstrated for vibration control at ship engines [16]. The most advanced concept is the application of an active dynamic control loop for the adjustment of the resonance frequency. The principle can be briefly explained with a TVA represented by a simple mechanical oscillator (**Figure 4**), which can be excited by an integrated actuation force F_A. The differential equation of this system reads:

$$m_N \ddot{x} + d \dot{x} + kx = F_A \tag{5}$$

where d is the damping coefficient and k is the stiffness of the oscillator. The feedback loop is closed by using the acceleration $\ddot{x}$ as the control input and the actuation force as output. If a simple proportional controller

$$G(s) = g \tag{6}$$

is applied, Eq. (5) can be reformulated to:

$$(m_N - g)\ddot{x} + d \dot{x} + kx = 0 \tag{7}$$

Thus, by feeding back forces proportional to the acceleration of the mass, the effective mass of the system can be altered. Similarly, by using an integral controller, a velocity feedback loop can be realized to adjust the damping of the system. In order to enhance the vibration absorption effect, active removal of system damping can be considered [8]. Also, a further integration can be implemented in order to obtain the position of the mass. By feeding back this signal, the stiffness of the absorber can be adjusted [17].

The frequency range that can be covered by the adaptation mechanism is a key performance parameter for an adaptive TVA. As studied in [15], the active control system is limited by the stability margins of the control loop. These margins are mainly defined by the inherent phase lag of many signal processing components, but also by the geometrical arrangement of the sensor and the actuator.

By applying an electrical shunt circuit to the piezoelectric element, the stiffness can be varied without using a sensor component [18]. By using active circuits to realize negative capacitances, a broad adaptation frequency range can be realized. However, the active circuits have
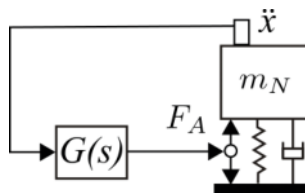
Figure 4. Feedback control to adjust the resonance frequency.

to be designed with respect to the high voltages that occur at the piezoelectric elements, which still remain a challenge [19].

2.3. Active systems with inertial mass actuators

2.3.1. Inertial mass actuators

Most versatile are active vibration control systems using dynamic actuation [20]. In this case, the force is generated by an inertial mass, which is excited by an active element. To enable a broad band actuation, the inertial mass is usually mounted with soft springs to the host structure, which causes a resonance in the system. Thus, the resulting force exciting the host structure exhibits a dynamic behavior, and the inertial mass actuator can be treated as a constant force generator only when being driven well above the resonance frequency. The frequency response of an inertial mass actuator with a mass m, resonance frequency ω_0, damping coefficient θ, and an internal actuation force F_A reads:

$$\frac{F(s)}{F_{A(s)}} = \frac{s^2}{s^2 + 2\theta\omega_0^2 s + \omega_0^2}.$$

(8)

A simple example of an inertial mass actuator with a resonance frequency of 10 Hz is shown in **Figure 5**.

Inertial mass actuators have been used for active vibration control in cars [21], trains [22], or building floors [23]. For very large structure like wind turbines actuation for the first dominating mode with a large force is required. Then, the concepts of the TMD and the inertial mass
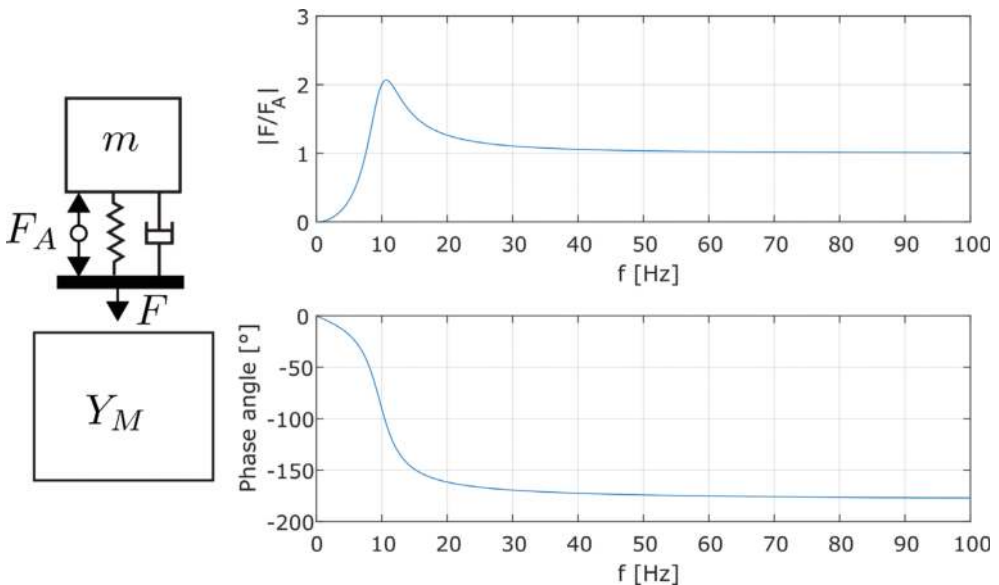
Figure 5. Basic model of an inertial mass actuator and its frequency response function.

actuator converge to the active tuned mass damper [24]. Recent developments also treat non-linearities in the host structures by extending the theoretical considerations for tuning of the system and the control law [26].

If the host structure is a non-linearly oscillating system, extended considerations are necessary in the design of those systems.

Mostly, electrodynamic actuation is preferred, because it enables a straightforward system design for a low resonance frequency.

Still, some work is dedicated to the integration of piezoelectric actuation. Since piezoelectric actuators possess very high resonance frequencies, proper designs have to be found that make such stiff actuators applicable for an oscillator with a low resonance frequency. However, the advantage of using piezoelectric actuation is the capability of the piezoelectric actuators to function as structural elements and partly carry the inertial mass, enabling compact systems with less movable parts.

Piezoelectric TVA systems can also be used in a hybrid mode. While being tuned to one resonance frequency, they can be actively driven at higher frequencies and work as inertial mass actuators [25].

2.3.2. Control methods

When the inertial mass actuator is driven well above its resonance frequency, it represents an ideal force generator. Thus, arbitrary active vibration control methods are applicable. Two basic concepts should be briefly repeated (**Figure 6**).

The feedback control system (**Figure 6**, left) is often applied to implement skyhook damping or other concepts which aim at influencing the characteristics of the host structure. Further details on control methods like velocity feedback or positive position feedback can be found in [27].

Feedforward control is usually implemented with adaptive digital filters [28]. The main field of application for active control of vibrations is narrowband or harmonic disturbance forces exciting the host structure. To compensate those, a reference signal with the same frequency is
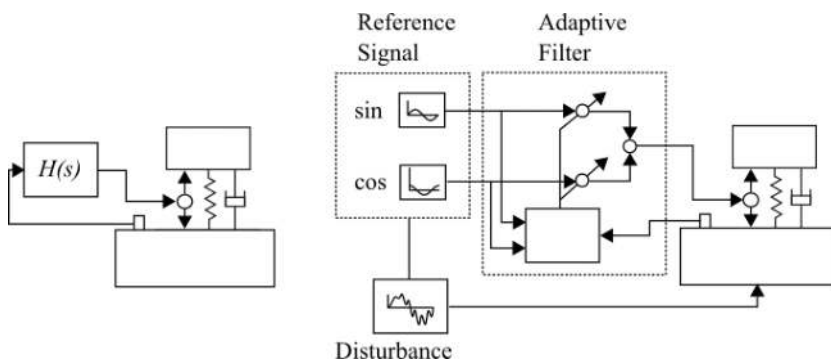
Figure 6. Feedback and feedforward control of an inertial mass actuator.

generated and filtered in order to match the phase angle and amplitude for an optimal suppression of the disturbance.

2.4. Comparison of the methods

To illustrate the characteristics of the introduced vibration control systems, the basic example (**Figure 1**) is used once more [7]. As disturbance, a harmonic excitation force of 1 N with slowly sweeping frequency between 40 and 60 Hz is considered. As a performance indicator, the RMS of the acceleration of the host structure is used. A passive TVA, an adaptive TVA, and an active system with an inertial mass actuator driven by an adaptive FXLMS algorithm are compared. The mechanical parameters of the different devices are summarized in (**Table 2**).

The result summarizing numerical simulations of all three configurations is presented in **Figure 7**. Obviously, the active system shows the best performance using just a moderate

System	Passive	Adaptive	Active
Resonance frequency [Hz]	50	50 (+/ 5Hz adaptation range)	10
Mass [kg]	0.5	0.1	0.1
Damping coefficient [−]	0.01	0.01	0.03

Table 2. Parameters of the compared vibration control systems (from [7]).
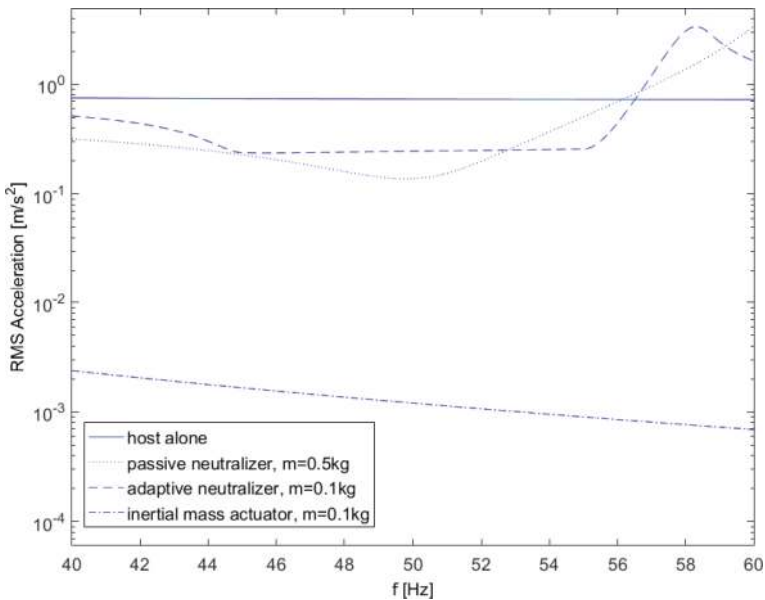
Figure 7. RMS acceleration of a vibrating host structure with different vibration control systems.

System	Passive	Adaptive	Active
Vibration reduction	Medium	Medium	High
System complexity	Low	Medium	High
Energy supply	None	During adaptation (depending to the concept)	Continuously
Added mass	High	Low	Low
Bandwidth	Low	Medium	High

Table 3. Comparison of passive, adaptive and active control systems.

additional mass, however at the expense of a complex system set up using digital signal processing and a dynamic actuation, which can cause issues when scaling the system for vibration control of very large structures. The adaptive and the passive vibration absorber cause similar vibration reduction; however, the passive system uses a five times higher mass than the adaptive (**Figure 7**).

Summarizing, the solution for an optimal vibration control system depends to the given vibration problem and the respective requirements and restrictions like allowed amount of added mass, possibility for energy supply, or the characteristics of the disturbance (**Table 3**).

This motivated the development of a vibration control system that can be used to realize passive, adaptive, and active vibration control systems, which will be introduced in the next section. This might be especially useful for prototyping purposes when an evaluation of different system concepts is needed. Furthermore, the system can be used to implement hybrid systems that combine passive, adaptive and active control.

3. Design of a hybrid piezoelectric absorber and inertial mass actuator

The vibration control device introduced here utilizes piezoelectric actuators due to their ability to carry high static mechanical loads while providing static and dynamic actuation forces. This should enable a multifunctional system. The design follows the well-known mechanical oscillator consisting of a bending beam as spring element and a tip mass. In parallel to the bending beam, two piezoelectric stack actuators are connecting the base and the tip mass (**Figure 6**).

In phase static actuation or static preloads by the screws apply tensile forces to the bending beam, which alters the stiffness and enables adaptation of the resonance frequency. Alternatively, out-of-phase dynamic operation of the piezoelectric actuators generates bending movements of the beam, which causes transverse dynamic forces at the base of the absorber. More details on the design can be found in [29, 30].

3.1. Adaptation by static preloading

The adaptation by static preloading can be described by the differential equation for the axially loaded Euler-Bernoulli beam:

$$EIw'''' + F_N w'' = 0 \tag{9}$$

Here, additional beam stiffness is generated by the tensile force F_N. This force can be provided mechanically by the preloading screws or electrically by applying static voltages to the piezo-electric actuators. To compute the tensile beam force, a serial connection of actuators and beam with the respective stiffness's k_A and $k_{N,b}$ has to be considered. The overall longitudinal stiffness $k_{N,eff}$ of this configuration is defined by:

$$k_{N,eff} = \frac{2k_A k_{N,b}}{2k_A + k_{N,b}} \tag{10}$$

Thus, for the mechanical preloading the force is evaluated by:

$$F_N = k_{N,eff} u_s \quad \text{with} \quad u_s = \eta \alpha \tag{11}$$

Hereby, the displacement of the screw u_s is defined by the product of their thread pitch η and turning angle α. For the electrical preloading the tensile force is calculated differently to Eq. (11):

$$F_N = k_{N,eff} u_{el} \quad \text{with} \quad u_{el} = d_{33} n_A U_{el} \tag{12}$$

The product of the electro-mechanical constant d_{33}, the number of actuator layers n_a and electrical voltage U_{el} yield to piezo actuator's displacement u_{el}.

To solve the aforementioned differential Eq. (9), an adequate trial function is chosen and the boundary conditions are defined. From this, follows the system of equations to be solved to gain the constants of the trial function [30].

Also, the effective transverse stiffness of the beam $k_{t,eff}$ w.r.t. to the position $x = l + a$ (refer to **Figure 8**) is derived from this solution:

$$k_{t,eff} = \left(\frac{w(x = l + a)}{F} \right)^{-1} \tag{13}$$

Considering a tip mass at position $x = l + a$, the natural frequency of the system can be evaluated depending on the tensile preload. In Section 3.3, the analytical and experimental results are compared. A good match is observed for both, mechanical and electrical tuning.

3.2. Generation of dynamic forces

As mentioned above, the piezo actuators can be used in dynamic operation (out of phase) to generate transverse forces. This enables the system to work as an inertial mass actuator at frequencies above its first natural frequency. To estimate the characteristics of the force F generated in transverse direction, a simplified analytical model with respect to the actuator force is used. Since the inertial mass at the tip is expected to be much heavier than the actuation unit depicted in **Figure 8**, the mass of the latter is neglected here in order to simplify the calculations using again the theory of the Euler beam. The system can be represented by a
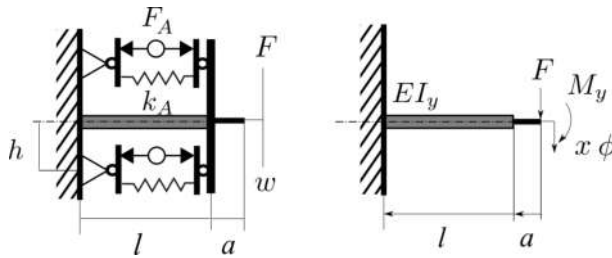
Figure 8. Mechanical model of the vibration control device.

bending beam with a tip force F and moment M_y. The respective tip displacement w and angle w' can be found too by solving Eq. (9). The moment M_y at the tip due to the actuator force F_A and the restoring force of the actuator stiffness k_A can be expressed by:

$$M_y = 2 \left(h\, F_A - k_A\, h^2\, w'(x = l) \right)$$ (14)

In order to include the geometry of the mass, the distance from the end of the beam to the center of gravity of the mass is defined by a (refer to **Figure 8**). In Eq. (15), the displacement $w(x = l + a)$ is evaluated

$$w(x = l + a) = w(x = l) + a\, w'(x = l)$$ (15)

The free stroke at this point due to the actuator force F_A can be calculated by setting the force F to zero and using the solution of Eq. (9) for $w(x = l)$ and $w'(x = l)$ and applying this to Eqs. (14) and (15).

In a similar manner, the stiffness $k = F/w$ can be calculated by setting $F_A = 0$. The block force of the actuator system can be calculated by multiplying the free stroke due to out-of-phase actuator excitation and the stiffness of the system:

$$F = k\, w(x = l + a)$$ (16)

Hence, considering a tip mass m at position $x = l + a$ all quantities are defined in order to calculate the dynamic behavior of the system due to actuator excitation.

3.3. Experimental characterization

According to the sketch (**Figure 9**) a prototype was built that is shown in **Figure 10**.

A thin beam is clamped between two steel blocks, which represents the mounting of the inertial mass actuator. The width of the beam is large compared to its length to prevent torsion. The whole pattern of the mounting is suited for a connection to a shaker, a heavy breadboard or the test structure addressed subsequently. On the other side of the beam, the inertial mass is attached. Two simple steel blocks are used to realize the clamping of the beam, which can be changed easily for experiments. For assembling the piezoelectric actuators the beam is
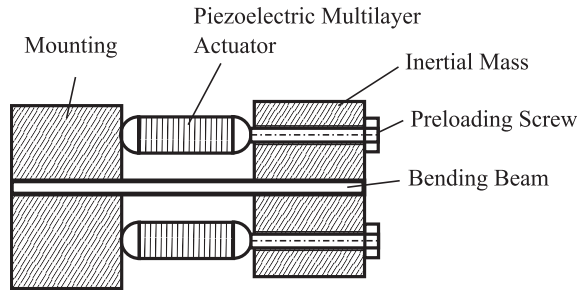
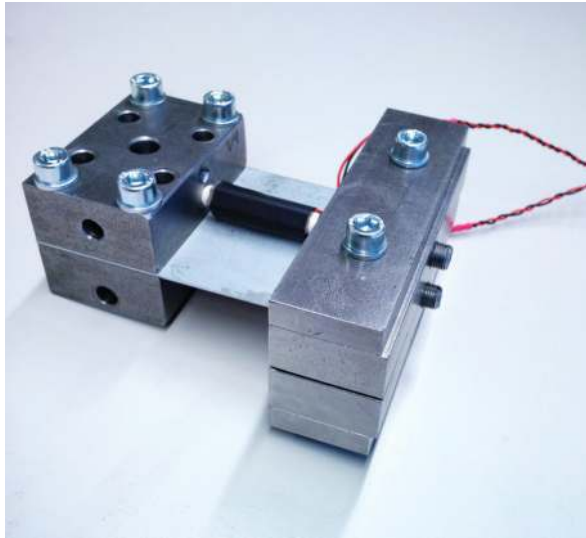**Figure 9.** Design of the vibration control device.

Figure 10. Implemented prototype of the adaptive vibration absorber/inertial mass actuator.

equipped with slotted holes. Monolithic multilayer actuators by CeramTec with a base area of 7.6×7.1 mm and a length of 30 mm are integrated. On both sides of the piezoelectric actuators, spherical ceramic caps are glued to reduce damaging bending and shear forces. To ensure the force transmission of the actuators and to avoid loosening and, therefore, the non-linear behavior, the actuators have to be pre-loaded. This is done by screws in the two masses next to the beam with a distance of 7.5 mm to the beam's surface. The tips of the pre-loading screws are concave as counterparts of the actuator's ceramic caps. There are corresponding holes at the mounting at the same distance from the beam. This prevents shifting of the piezoelectric actuators in operation. The parameters for the actuator system are depicted in **Table 4**.

Quantity	Symbol	Value	Unit
Beam			
Length	l	41.5	mm
Width	b	60	mm
Thickness	d	0.5	mm
Young's modulus	E	$2.2 \cdot 10^{11}$	N/m^{-2}
Mass			
Mass	m	1.078	kg
Actuator			
Stiffness	k_A	$42 \cdot 10^6$	Nm^{-1}
Max. block force	$F_{B,max.}$	2000	N

**Table 4.** Parameters of the actuator systems.

3.3.1. Adaptation of the resonance frequency by static preloads

To analyze the dynamic characteristics of the inertial mass actuator, tests were performed. The whole actuator was mounted to a rigid, heavy base plate which can be treated as an infinitely small mechanical admittance in the considered frequency range (**Figure 11**). The tip mass was instrumented with an accelerometer and excited by an impulse hammer in order to gain the resonance frequencies by evaluating the respective frequency response functions depending on both conditions—mechanical and electrical preload.

Exemplarily the frequency responses for electrical tuning are depicted in **Figure 12**. Obviously, the effect of preloading is significant and has to be taken into account. The analytical model which is introduced in the preceding section is validated by the experimental results. Some differences between experimental and analytical frequency responses can be observed for very low DC voltages, where the absorber does not exhibit perfect characteristics of a single-degree-of-freedom oscillator. This could be caused by a poor mechanical coupling between the piezo stacks and the structure when nearly no pre-load is applied. For very high pre-loads around 140 V, the model predicts higher tuning effects than measured in the experiment (**Figure 12**). In this case, the analytical model might not perfectly predict the contact characteristics of the ball joints, which can be non-linear for high mechanical loads.

The comparison of the measured and the calculated resonance frequencies is shown in **Figure 13** for both cases (mechanical and electrical tuning). By mechanical preloading a larger frequency shift compared to electrical preloading is realized. This can be explained by the limited blocking force of the piezo actuators. However, a good match between the experimental values for the resonance frequencies and the calculated results is observed for both cases.

The performance of both tuning concepts is comparable to adaptive absorbers, which use motors for the variation of the spring geometry investigated in preliminary work [15].
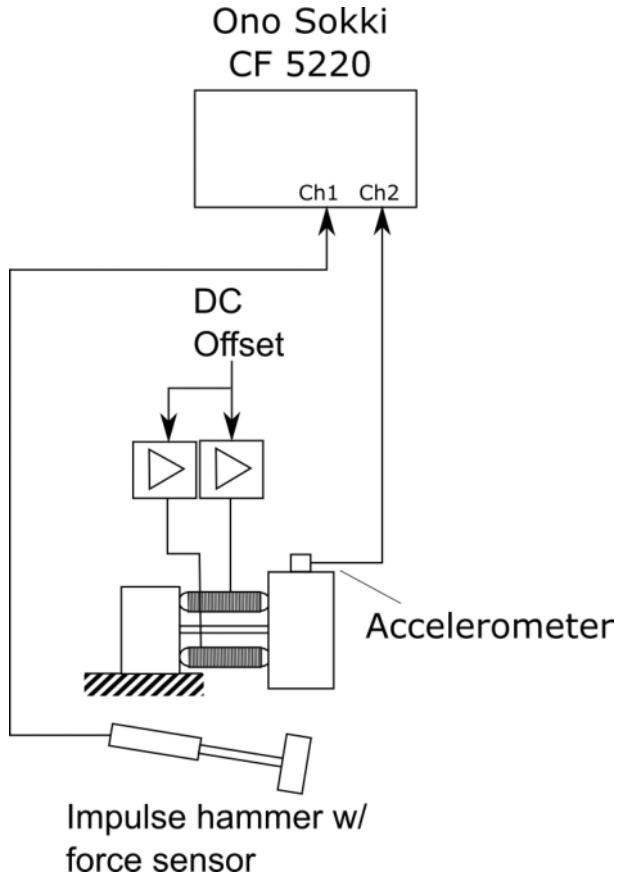
Figure 11. Test set up for the dynamic analysis of the adaptive vibration absorber.
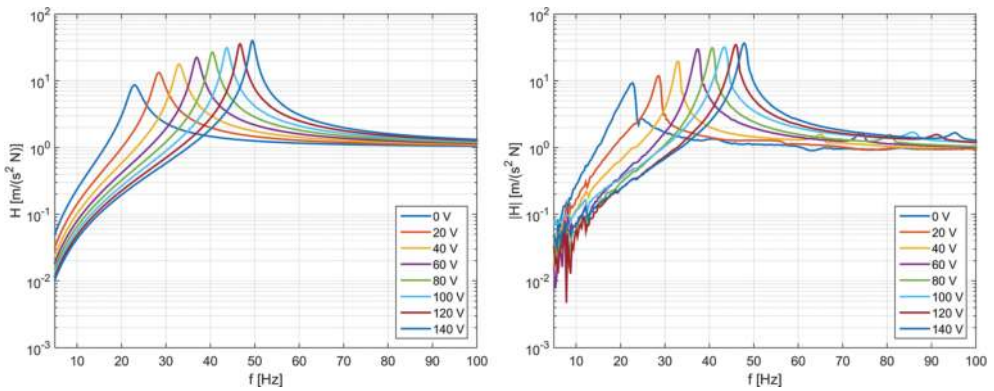
Figure 12. Frequency response functions of the adaptive vibration absorber for different DC voltages (electrical tuning) - simulation results (left) and experimental results (right).

3.3.2. Dynamic force generation

For the evaluation active force generated by the device, the piezoelectric actuators were driven with a swept sine signal by the analyzer. A simple analogue circuit realizes an out of phase driving signal for one of the actuators in order to excite the bending mode of the actuator system to produce transverse forces, and the acceleration of the tip mass was measured (**Figure 14**). Since the mounting can be assumed to be rigid, the block force can be directly derived from the acceleration and the mass.
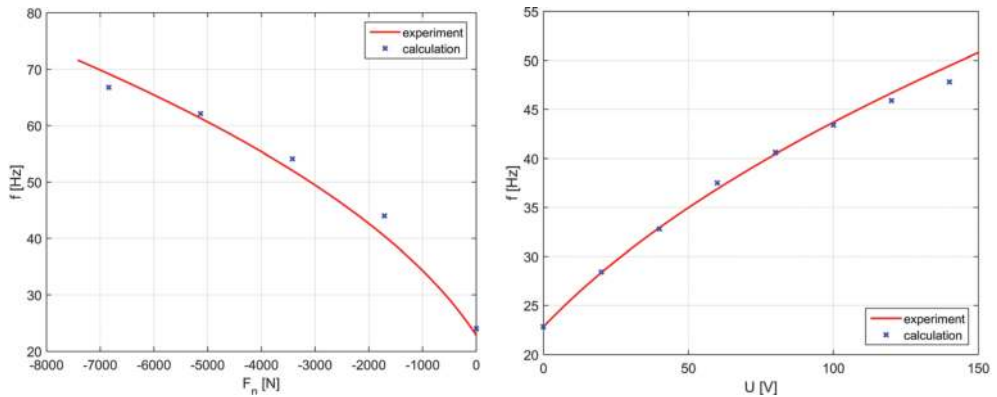

Figure 13. Variation of resonance frequency by mechanical (left) and electrical preloading (right).
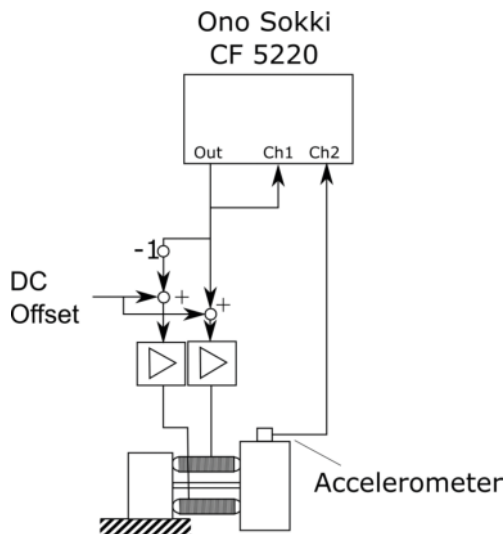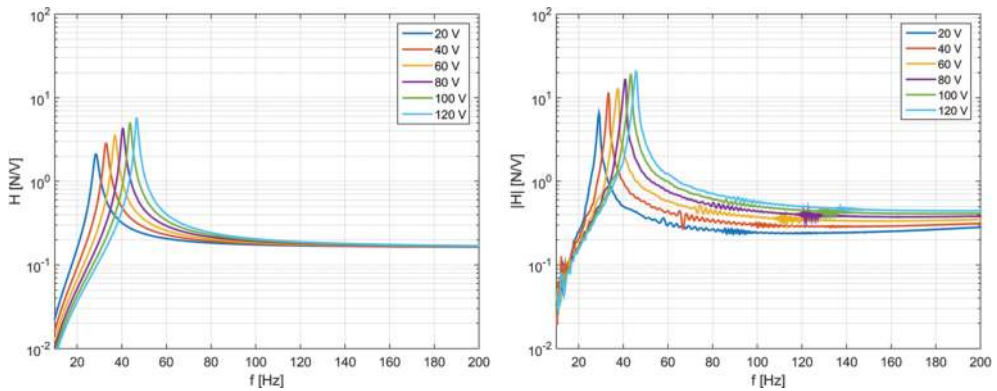

Figure 14. Test set up for the measurement of the dynamic block force of the actuator.

Figure 15. Calculation (left) and measurement (right) of the dynamic block force of the actuator.

For this test, different preloads from 20 to 120 V_{DC} were applied to the actuators. The resulting frequency responses between applied driving voltage and the generated force show the expected characteristics (**Figure 15**).

In the frequency range above the first resonance and 250 Hz, no further resonances are excited. However, it was observed that, compared to the analytical frequency responses, the measured ones are influenced by the pre-load. Additionally, the block force is underestimated by the analytical frequency responses. Above the resonance the block force increases slightly with the pre-loading voltage. This might be caused by a non-linearity in the piezoelectric elements, i.e., a dependency of the piezoelectric constant to the pre-load. In the next section, the application of the actuator system to a truss structure is conducted. Therefore, the adaptive and active mode of the actuator system is used simultaneously in order to attenuate unwanted vibration in different frequency regions.

4. Application to an elastic truss structure

To evaluate the performance in an active vibration control system, the actuator was mounted to a lightweight truss structure (**Figure 16**). The actuator was instrumented with accelerometers at its base and at the inertial mass.

In the first step, the adaptive absorber was tuned by mechanical pre-load to a structural mode, which resulted in a vibration absorption effect at 43 Hz (**Figure 17**). This effect was enhanced by choosing an additional electrical pre-load of 50 V_{DC}, which resulted in an absorption frequency of 50 Hz. Although this frequency does not match the structural resonance at 48 Hz exactly, this configuration served well as a basis for adjusting the active control system.

In the next step, the active control system was set up and tuned. Two control loops were implemented successively and connected (**Figure 18**). First, an active velocity feedback loop $H_v(s)$ was used to enhance the damping of the inertial mass actuator, which caused the better

Figure 16. Test set up for the active control experiment (left) and detail of the actuator instrumentation (right).
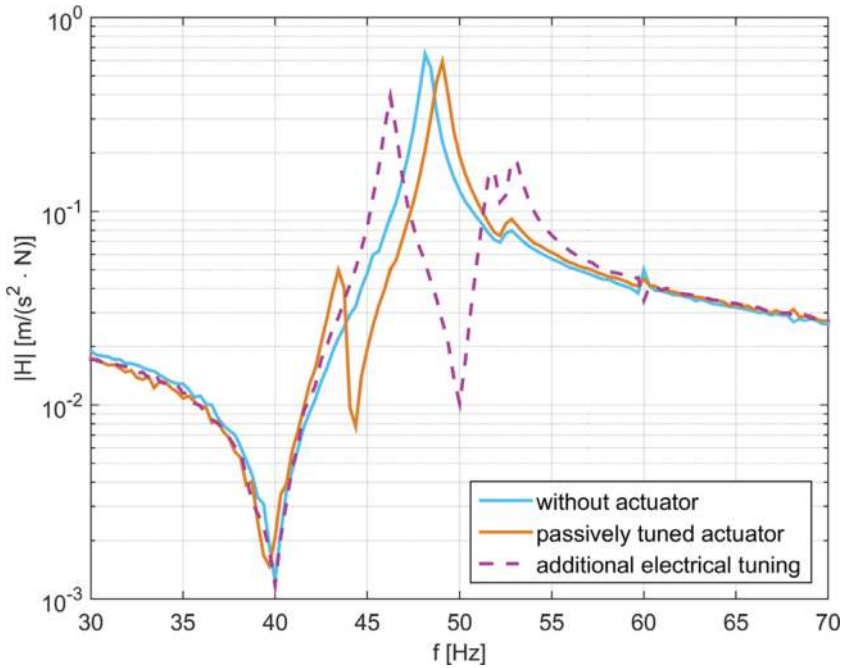

Figure 17. Tuning of the adaptive absorber to the first elastic mode of the truss.

performance of the absorption at the first mode at 48 Hz and a higher robustness against the interaction between different control loops. In order to derive the dynamic velocity from the measured acceleration at the tip mass, an integrator is used. In a practical control system, this is implemented with a low pass filter:

$$H_v(s) = \frac{g_v}{s + \omega_{LP}}$$ (17)

The cut-off frequency ω_{LP} is set well below the resonance of the actuator, here at about 5 Hz, and g_v is chosen appropriately. Second, an acceleration feedback loop was tuned to the second
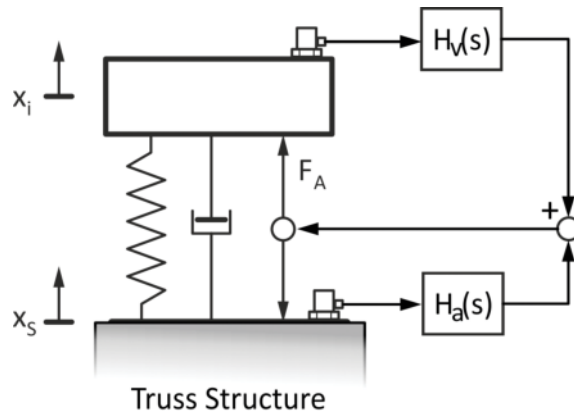

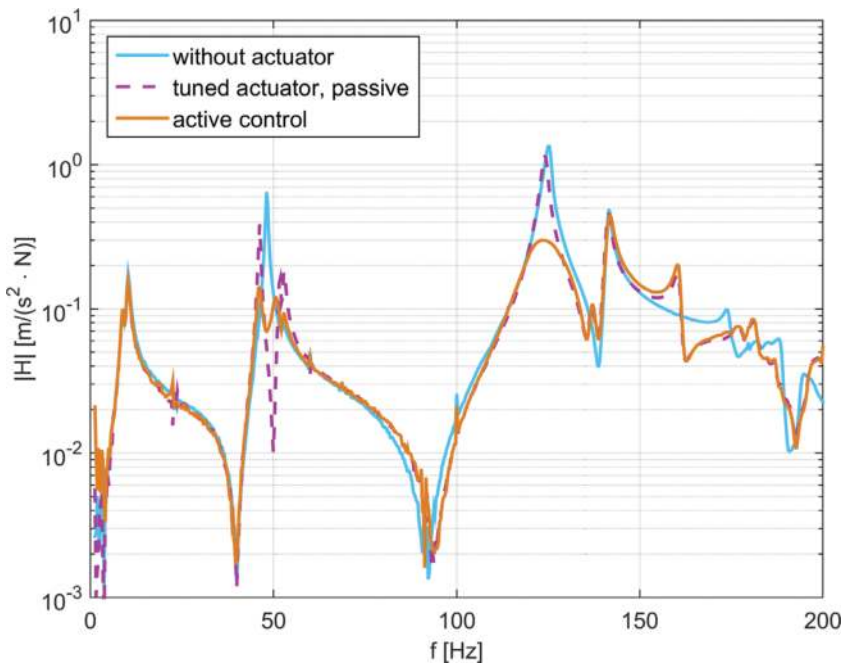**Figure 18.** Block diagram of the control system.

Figure 19. Control results for the truss structure.

mode of the truss at 125 Hz (**Figure 19**). The corresponding transfer function is a second order low pass filter:

$$H_a(s) = \frac{g_a \omega_c}{s^2 M + 2\theta\, \omega_c\, s + \omega_c^2} \tag{18}$$

Here, ω_c is the tuning frequency and θ the damping coefficient, while g_a is the control loop gain. The control system was implemented with analog circuitry.

Since the actuator is not symmetric, a bending moment is exciting at its base additional to the transverse force. This results in lowering of a higher resonance frequency from 180 to 160 Hz and a deterioration of the vibration amplitudes in this frequency region.

5. Conclusions

Adaptive and active vibration control systems can outperform passive systems in terms of additional mass and vibration reduction. However, the different systems cause an increase of system complexity and need for additional power supply. Thus, alternative feasible approaches should be evaluated to find the optimal solution for a given vibration problem. To enable experimental prototyping, a design for a TVA has been introduced, that can be used for passive, adaptive, and active vibration control. It has also been shown that an advantage of such an integrated system can be applied to hybrid systems that work as passive absorbers in the lower frequency range and a can excite active forces at higher frequencies.

Author details

Dirk Mayer* and Sven Herold

*Address all correspondence to: dirk.mayer@lbf.fraunhofer.de

Fraunhofer Institute for System Reliability and Structural Durability LBF, Darmstadt, Germany

References

[1] Frahm H. Device for Damping Vibrations of Bodies; United States Patent US 989958A, 1911

[2] den Hartog JP. Mechanical Vibrations. New York: Dover Publications, Inc., 1985

[3] Debnath N, Deb S, Dutta A. Multi-modal vibration control of truss bridges with tuned mass dampers under general loading. Journal of Vibration and Control. 2016;**22**(20):1-20. DOI: 10.1177/1077546315571172

[4] Kegerise M, Cattafesta L, Ha C-S. Adaptive identification and control of flow-induced cavity oscillations. In: 1st Flow Control Conference; 24–26 June 2002. DOI: 10.2514/6.2002-3158

[5] Chung J. Vibration absorber for reduction of the in-plane vibration in an optical disk drive. IEEE Transactions on Consumer Electronics. 2004;**50**:552-557. DOI: 10.1109/TCE.2004.1309422

[6] McGoldrick RT. Ship Vibration: Report. Vol. 1451. Washington, DC: David Taylor Model Basin—Department of the Navy; 1960

[7] Gardonio P, Brennan MJ. On the origins and development of mobility and impedance methods in structural dynamics. Journal of Sound and Vibration. 2002;**249**:557-573. DOI: 10.1006/jsvi.2001.3879

[8] Kidner M, Brennan MJ. Improving the performance of a vibration neutraliser by actively removing damping. Journal of Sound and Vibration. 1999:587-606

[9] Soto MG, Adeli H. Optimum tuning parameters of tuned mass dampers for vibration control of irregular highrise building structures. Journal of Civil Engineering and Management. 2014;**20**:609-620. DOI: 10.3846/13923730.2014.967287

[10] Mayer D, Herold S, Kauba M, Koch T. Approaches for distributed active and passive vibration compensation. In: Proceedings of ISMA 24, 20.-22.09.2010, Leuven, Belgium, pp. 581-593

[11] Brennan MJ. Some recent developments in adaptive tuned vibration absorbers/neutralisers. Shock and Vibration. 2006;**13**:531-543. DOI: 10.1155/2006/563934

[12] Bonello P. Adaptive tuned vibration absorbers: Design principles, concepts and physical implementation. In: Beltran-Carbajal F, editor. Vibration Analysis and Control—New Trends and Developments. Rijeka, Croatia: InTech; 2011

[13] Wright RI, Kidner MRF. Vibration absorbers: A review of applications in interior noise control of propeller aircraft. Journal of Vibration and Control. 2004;**10**:1221-1237. DOI: 10.1177/1077546304041368

[14] Kela L, Vähäoja P. Recent studies of adaptive tuned vibration absorbers/neutralizers. Applied Mechanics Reviews. 2009;**62**:60801. DOI: 10.1115/1.3183639

[15] Mayer D, Pfeiffer T, Vrbata J, Melz T. Adaptive-passive vibration control systems for industrial applications. SPIE Smart Structures and Materials + Nondestructive Evaluation and Health Monitoring; 8 March 2015. SPIE; 2015. p. 94330E. DOI: 10.1117/12.2086359

[16] Howard CQ. Recent developments in submarine vibration isolation and noise control. In: Proceedings of the 1st Submarine Science Technology and Engineering Conference; 2011

[17] Hassan A, Torres-Perez A, Kaczmarczyk S, Picton P. Vibration control of a Stirling engine with an electromagnetic active tuned mass damper. Control Engineering Practice. 2016;**51**:108-120. DOI: 10.1016/j.conengprac.2016.03.014

[18] Davis CL, Lesieutre GA. An actively tuned solid-state vibration absorber using capacitive shunting of piezoelectric stiffness. Journal of Sound and Vibration. 2000;**232**:601-617. DOI: 10.1006/jsvi.1999.2755

[19] Heuss O, Salloum R, Mayer D, Melz T. Tuning of a vibration absorber with shunted piezoelectric transducers. Archive of Applied Mechanics. 2016;**86**:1715-1732. DOI: 10.1007/s00419-014-0972-5

[20] Winberg M, Johansson S, Claesson I. Inertial mass actuators—Understanding and tuning. In: Proceedings ICSV 11; St. Petersburg; 2004

[21] Belgacem W, Berry A, Masson P. Active vibration control on a quarter-car for cancellation of road noise disturbance. Journal of Sound and Vibration. 2012;**331**:3240-3254. DOI: 10.1016/j.jsv.2012.02.030

[22] Persson P, Lagö TL, Norberg A. Active control of sleeper-induced sound in a high speed train (Conference Paper by Per Persson, Thomas L Lagö, Arvid Norberg)—Electronic Research Archive @ Blekinge Institute of Technology (BTH); 1999

[23] Díaz IM, Reynolds P. Robust saturated control of human-induced floor vibrations via a proof-mass actuator. Smart Materials and Structures. 2009;**18**:125024. DOI: 10.1088/0964-1726/18/12/125024

[24] Rahman M, Ong ZC, Chong WT, Julai S, Khoo SY. Performance enhancement of wind turbine systems with vibration control: A review. Renewable and Sustainable Energy Reviews. 2015;**51**:43-54. DOI: 10.1016/j.rser.2015.05.078

[25] Konstanzer P, Grünewald M, Jänker P, Storm S. Piezo tuneable vibration absorber system for aircraft interior noise reduction. In: Proceedings of Euronoise 2006; 30 May–01 June 2006; Tampere, Finland. 2006

[26] Beltrán-Carbajal F, Silva-Navarro G. Active vibration control in Duffing mechanical systems using dynamic vibration absorbers. Journal of Sound and Vibration. 2014;**333**:3019-3030

[27] Preumont A. Vibration Control of Active Structures: An Introduction. 3rd ed. Berlin, Heidelberg, NewYork, Hong Kong, London, Milan, Paris, Tokyo: Springer; 2011

[28] Kuo SM, Lee BH. Real-Time Digital Signal Processing. New York, Chichester: Wiley; 2001

[29] Herold S, Mayer D, Melz T, Röglin T. Design and test of a piezoelectric inertial mass actuator for active vibration control. In: Sinha J, editor. Vibration Engineering and Technology of Machinery. 23rd ed. United Kingdom: Springer International Publishing; 2014. pp. 587-597

[30] Herold S, Mayer D. Adaptive piezoelectric absorber for active vibration control. Actuators. 2016;**5**:7. DOI: 10.3390/act5010007